Abdominal Imaging

© Springer Science+Business Media New York 2015
Published online: 19 May 2015

Abdom Imaging (2015) 40:2323–2330
DOI: 10.1007/s00261-015-0447-3

Simultaneous Multislice Accelerated Free-Breathing Diffusion-Weighted Imaging of the Liver at 3T

Chika C. Obele,[1] Christopher Glielmi,[2] Justin Ream,[1] Ankur Doshi,[1] Naomi Campbell,[1,3] Hoi Cheung Zhang,[1] James Babb,[1] Himanshu Bhat,[4] Hersh Chandarana[1]

[1]Department of Radiology, New York University Langone Medical Center, 660 First Avenue, New York, NY 10016, USA
[2]Siemens HealthCare, New York, NY, USA
[3]Department of Radiology, Memorial Sloan Kettering, New York, NY, USA
[4]Siemens HealthCare, Charlestown, MA, USA

Abstract

Purpose: To perform image quality comparison between accelerated multiband diffusion acquisition (mb2-DWI) and conventional diffusion acquisition (c-DWI) in patients undergoing clinically indicated liver MRI. *Methods*: In this prospective study 22 consecutive patients undergoing clinically indicated liver MRI on a 3-T scanner equipped to perform multiband diffusion-weighed imaging (mb-DWI) were included. DWI was performed with single-shot spin-echo echo-planar technique with fat-suppression in free breathing with matching parameters when possible using c-DWI, mb-DWI, and multiband DWI with a twofold acceleration (mb2-DWI). These diffusion sequences were compared with respect to various parameters of image quality, lesion detectability, and liver ADC measurements. *Results*: Accelerated mb2-DWI was 40.9% faster than c-DWI (88 vs. 149 s). Various image quality parameter scores were similar or higher on mb2-DWI when compared to c-DWI. The overall image quality score (averaged over the three readers) was significantly higher for mb-2 compared to c-DWI for $b = 0$ s/mm^2 (3.48 ± 0.52 vs. 3.21 ± 0.54; $p = 0.001$) and for $b = 800$ s/mm^2 (3.24 ± 0.76 vs. 3.06 ± 0.86; $p = 0.010$). Total of 25 hepatic lesions were visible on mb2-DWI and c-DWI, with identical lesion detectability. There was no significant difference in liver ADC between mb2-DWI and c-DWI ($p = 0.12$). Bland–Altman plot demonstrates lower mean liver ADC with mb2-DWI compared to c-DWI (by 0.043×10^{-3} mm^2/s or 3.7% of the average ADC). *Conclusion*: Multiband technique can be used to increase acquisition speed nearly twofold for free-breathing DWI of the liver with similar or improved overall image quality and similar lesion detectability compared to conventional DWI.

Key words: Liver MRI—Diffusion-weighted imaging—Simultaneous multislice acceleration DWI—Multiband DWI

Diffusion-weighted imaging (DWI) is commonly used in the abdomen, particularly in the evaluation of focal and diffuse liver diseases, with promising results [1–7] DWI is relatively easy to implement in clinical practice and can be incorporated into the existing MR protocols. Thus it has become an integral component of liver MRI protocol at our institution and at many others.

Single-shot spin-echo echo-planar (SS EPI) technique with fat-suppression is most frequently used acquisition scheme for liver DWI. Liver SS EPI DWI acquisition can be performed in a breath-hold or in free breathing with either multiple signal-averaging to reduce the effects of motion or with respiratory and/or cardiac triggering. Each acquisition scheme has potential advantages and disadvantages [8]. Although breath-hold DWI acquisition is fast, the need to acquire the data within a breath-hold limits signal-to-noise, volumetric coverage, resolution, and number of b values that can be acquired. Free-breathing DWI can overcome many of the above limitations but at the expense of longer acquisition time [7, 9–12]. Several studies have demonstrated good reproducibility of ADC measurements with free-breathing acquisition [13, 14], and the ADC measurements with the free-breathing have also been demonstrated to be more

Correspondence to: Hersh Chandarana; *email:* hersh.chandarana@nyumc.org

reproducibility with less scatter compared to the respiratory triggered DWI in some studies [14]. The reason for the higher robustness of free-breathing DWI compared to navigator triggered acquisition is unclear but hepatic pseudo-anisotropy has been proposed as one potential cause of less ADC reproducibility in navigator trigger liver imaging [14, 15]. A recent study recommended free-breathing technique for liver diffusion-weighted imaging because of similar reproducibility and shorter acquisition time compared to multiple breath holds or respiratory navigator triggered techniques [13].

Technique that can accelerate free-breathing DWI of the liver is of interest to decrease acquisition time while maintaining high image quality. One promising method is multiband excitation approach that can acquire multiple slices simultaneously [16–18], in contrast to current EPI sequences which acquires single slice at a time. Multiband approach can decrease the repetition time or TR and has been shown to accelerate DWI in brain [18], but has not been systematically evaluated for accelerated liver imaging. Therefore, the purpose of this prospective study was to perform image quality comparison between accelerated multiband diffusion acquisition (mb2-DWI) and conventional diffusion acquisition (c-DWI) in patients undergoing clinically indicated liver MRI.

Methods

Two of the authors CG and HB are employees of Siemens HealthCare. However, Siemens HealthCare provided no financial support for this study, and the remaining authors had full control over all study data.

Subjects

This prospective study was HIPAA compliant and approved by our institutional review board. All subjects supplied written informed consent. Between January 2014 and March 2014, 22 consecutive patients (12 men and 10 female) with mean age of 56 years (range 33 to 83 years) undergoing clinically indicated liver MRI on a 3 T scanner equipped to perform mb-DWI agreed to participate in the study and constituted our study cohort. Indications for MRI were as follows: known or suspected history of hepatocellular carcinoma ($n = 7$); cirrhosis ($n = 7$); evaluation of suspected or known focal liver lesion ($n = 3$); abnormal liver enzymes ($n = 5$).

MR imaging

All patients underwent liver MRI on a clinical 3-T system with peak amplitude of 45 mT/m and a slew rate of 200 T/m/s (MAGNETOM Skyra, Siemens HealthCare, Erlangen, Germany). Scans were performed using an 18-channel body matrix receive coil. All patients underwent routine liver protocol that included coronal T2-weighted half-Fourier single-shot turbo spin-echo (HASTE), transverse T2 fat-saturated turbo spin echo, transverse T1-weighted gradient echo in- and opposed phase, and transverse 3D T1-weighted fat-suppressed gradient echo (volume interpolated breath-hold exam—VIBE) pre- and post-contrast acquisitions. DWI acquisitions were performed prior to contrast administration as detailed below.

DWI

Transverse free-breathing single-shot echo-planar (EP) acquisitions with monopolar tri-directional trace-weighting diffusion gradients was performed prior to contrast administration with matching parameters such as matrix, voxel size, and *b* values. Same frequency selective fat saturation was employed for the following 3 acquisition schemes.

Conventional DWI (c-DWI): TR/TE 4500/66 ms, matrix 164 × 123, voxel size (interpolated) 2.3 × 2.3 × 5 mm, 34 axial 5 mm slices with inter-slice gap of 0.5 mm, bandwidth 1386 Hz/pix, parallel imaging factor of 2, 3 *b* values (0, 400, and 800 s/mm^2), and 4 averages. Acquisition time 2:29 min (149 s).

Multiband DWI without accelerating (mb-DWI): TR/TE 4500/66 ms, matrix 164 × 123, voxel size (interpolated) 2.3 × 2.3 × 5 mm, 34 axial 5 mm slices with inter-slice gap of 0.5 mm, bandwidth 1386 Hz/pix, parallel imaging factor of 2, 3 *b* values (0, 400, and 800 s/mm^2), and 4 averages. Acquisition time 2:33 min (153 s).

Multiband DWI with twofold acceleration (mb2-DWI): Same multiband sequence as above was utilized with same acquisition parameters but with decrease in TR to 2400 ms and total acquisition time of 1:28 min (88 s). Two slices were acquired simultaneously (Fig. 1) using blipped CAIPIRINHA (slice shift = FOVphase/3) and individual slices are reconstructed using slice GRAPPA reconstruction [18].

Image analysis

Sequence and patient related information was removed for all three DWI sequences in 22 patients. Thus 66 de-identified diffusion-weighted acquisitions were presented in a random order to three board-certified radiologists who evaluated images independently and in blinded fashion. For each sequence *b* 0 and highest *b* value ($b = 800$ s/mm^2) images were assessed for following parameters of image quality using a scale of 1–5, with the highest score indicating the most desirable exam: overall image quality, clarity of intrahepatic vessels, sharpness of the posterior right hepatic lobe edge, conspicuity of the left lobe, and absence of respiratory motion artifact (Table 1). Furthermore, each reader noted presence or absence of a lesion on the review of diffusion-weighted

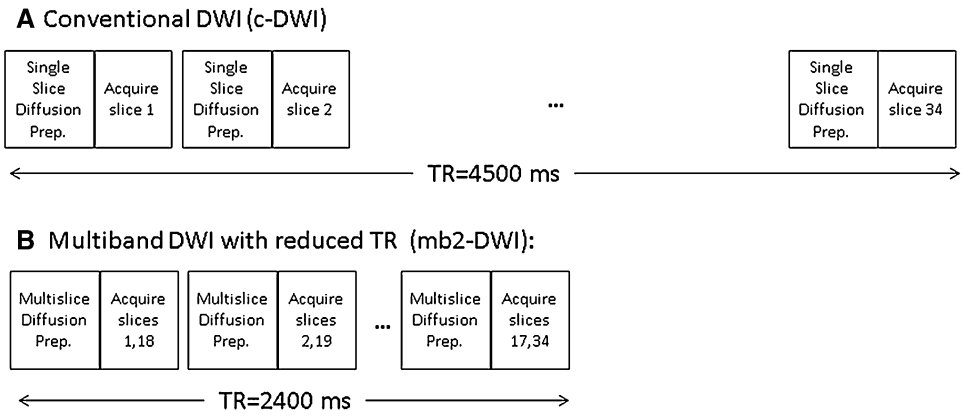

Fig. 1. Schema of the conventional (c-DWI) and accelerated multiband diffusion-weighted acquisition (mb2-DWI). Diffusion preparation includes diffusion encoding, multiband or single slice excitation, and refocusing pulse.

Table 1. Scoring system for Image quality parameters

Image quality parameters	Score	Scoring system
Overall image quality	1–5	1 = non-diagnostic; 2 = poor; 3 = fair; 4 = good; 5 = excellent
Clarity of intrahepatic vessels	1–5	1 = non-diagnostic; 2 = poor; 3 = fair; 4 = good; 5 = excellent
Sharpness of the posterior right hepatic lobe edge	1–5	1 = non-diagnostic; 2 = poor; 3 = fair; 4 = good; 5 = excellent
Conspicuity of the left lobe	1–5	1 = non-diagnostic; 2 = poor; 3 = fair; 4 = good; 5 = excellent
Absence of respiratory motion artifact	1–5	1 = non-diagnostic; 2 = poor; 3 = fair; 4 = good; 5 = excellent

images. If lesion was present this was marked and the image number was recorded.

Reader blinded to the acquisition scheme, placed round regions of interests (ROI) with average diameter 2–4 cm in the right lobe of the liver (avoiding the lesions and blood vessels) on three consecutive trans-axial slices on the $b = 0$ and $b = 800$ s/mm^2 to measure signal intensity (SI) on the DWI. This SI on the three consecutive slices was averaged to calculate average SI of the liver for each acquisition scheme.

The reader blinded to the acquisition scheme also placed a round region of interest with an average diameter of 4 cm in the right lobe of the liver on the ADC maps which were generated in-line at the scanner with monoexponential fitting of signal-intensities at all b values. Mean ADC values were recorded for each acquisition.

Statistical analysis

The mean and standard deviation for each image quality parameter for each reader was calculated. These image quality parameters were compared between the 3 DWI schemes using exact paired Wilcoxon signed-rank tests from each reader and for scores represented for each subject as an average over the three readers (denoted as AVERAGE). Inter-reader agreement of the qualitative measures was also computed using weighted kappa coefficients and classified as follows 0–0.20, slight agreement; 0.21–0.40, fair agreement; 0.41–0.60, moderate agreement; 0.61–0.80, substantial agreement; 0.81–1.00, almost perfect agreement [19]. SI was compared for $b = 0$ and $b = 800$ s/mm^2 between the three different sequences using paired t test. Bland–Altman Analysis was performed to compare ADC obtained with the three different sequences. All comparisons are two-sided and considered statistically significant at $p < 0.05$. Statistical computations except for Bland–Altman analysis were performed using SAS, version 9.3, SAS Institute, Cary, North Carolina. Bland–Altman Analysis was performed using MedCalc version 9.1 (MedCalc Software, Ostend, Belgium).

Results

Qualitative assessment

Scores for various image quality parameters for each reader and averaged over the three readers for the three DWI sequences for $b = 0$ and $b = 800$ s/mm^2 acquisitions are as noted in Tables 2 and 3, respectively. The inter-reader agreement (kappa) between the three readers for the various qualitative imaging parameters for the three sequences ranged from 0.12 to 0.56.

Acquisition time of the conventional (c-DWI) and multiband sequence without acceleration (mb-DWI) were similar, 149 vs. 153 s, respectively. However, multiband with acceleration factor of 2 (mb2-DWI) had acquisition time of 88 s, which was 40.9% faster than c-DWI and 42.5% faster than mb-DWI.

Multiband with acceleration of 2 (mb-2) vs. conventional DWI (c-DWI)

The overall image quality score (averaged over the three readers) was significantly higher for mb-2 compared to c-DWI for $b = 0$ s/mm^2 (3.48 ± 0.52 vs. 3.21 ± 0.54;

Table 2. Image quality parameters of $b = 0$ s/mm^2 images for the three diffusion sequences stratified by the reader and also averaged over the three readers

	mb2-DWI	mb-DWI	c-DWI
Overall image quality			
Average*	3.48 ± 0.52	3.33 ± 0.62	3.21 ± 0.54
Reader 1*	3.86 ± 0.47	3.64 ± 0.58	3.41 ± 0.67
Reader 2	3.05 ± 0.58	2.91 ± 0.75	2.86 ± 0.64
Reader 3	3.55 ± 0.91	3.45 ± 1.01	3.36 ± 0.85
Clarity intrahepatic vessels			
Average	3.06 ± 0.79	3.08 ± 0.82	2.92 ± 0.62
Reader 1	3.41 ± 0.67	3.32 ± 0.78	3.14 ± 0.64
Reader 2	2.64 ± 0.85	2.64 ± 1.00	2.50 ± 0.74
Reader 3	3.14 ± 1.21	3.27 ± 1.16	3.14 ± 1.04
Sharpness right lobe			
Average	3.80 ± 0.79	3.76 ± 0.71	3.61 ± 0.72
Reader 1*	4.45 ± 0.86	4.32 ± 0.99	4.00 ± 0.87
Reader 2	3.18 ± 0.91	3.14 ± 0.83	3.00 ± 0.87
Reader 3	3.77 ± 0.97	3.82 ± 0.91	3.82 ± 0.73
Conspicuity left lobe			
Average	3.53 ± 0.63	3.50 ± 0.63	3.48 ± 0.62
Reader 1*	3.68 ± 0.72	3.55 ± 0.67	3.36 ± 0.66
Reader 2	3.55 ± 0.74	3.59 ± 0.67	3.64 ± 0.79
Reader 3	3.36 ± 1.09	3.36 ± 1.00	3.45 ± 0.91
Motion robustness			
Average$^+$	3.20 ± 0.52	3.06 ± 0.49	3.11 ± 0.44
Reader 1	3.73 ± 0.46	3.68 ± 0.57	3.73 ± 0.55
Reader 2	2.59 ± 0.73	2.50 ± 0.80	2.41 ± 0.59
Reader 3	3.27 ± 0.88	3.00 ± 0.98	3.18 ± 0.91

* Multiband DWI with acceleration factor of 2 (mb2-DWI) had significantly higher score for overall image quality compared to conventional DWI (c-DWI) for scores averaged over three readers ($p = 0.001$) and for reader 1 ($p = 0.004$). For reader 1, score for right lobe sharpness ($p = 0.004$) and conspicuity of the left lobe ($p = 0.016$) were also significantly higher with mb2-DWI compared to c-DWI. There were no other significant differences ($p > 0.05$) between mb2-DWI and c-DWI

$^+$Average score for motion robustness was higher with mb2-DWI compared to multiband DWI (mb-DWI) ($p = 0.035$). There were no other significant differences between mb2-DWI and mb-DWI ($p > 0.05$)

Table 3. Image quality parameters of $b = 800$ s/mm^2 images for the three diffusion sequences stratified by the reader and also averaged over the three readers

	mb2-DWI	mb-DWI	c-DWI
Overall image quality			
Average*	3.24 ± 0.76	3.23 ± 0.68	3.06 ± 0.86
Reader 1*	3.64 ± 0.66	3.64 ± 0.58	3.32 ± 0.89
Reader 2	3.00 ± 0.69	2.91 ± 0.75	2.77 ± 0.75
Reader 3	3.09 ± 1.15	3.14 ± 1.13	3.09 ± 1.31
Clarity intrahepatic vessels			
Average	2.77 ± 0.98	2.79 ± 0.96	2.70 ± 0.96
Reader 1	3.00 ± 1.02	3.00 ± 0.87	2.82 ± 1.01
Reader 2	2.68 ± 0.99	2.59 ± 1.14	2.41 ± 1.01
Reader 3	2.64 ± 1.29	2.77 ± 1.11	2.86 ± 1.17
Sharpness right lobe			
Average	3.76 ± 1.00	3.68 ± 0.91	3.61 ± 1.04
Reader 1*	4.45 ± 1.10	4.36 ± 1.00	4.09 ± 1.23
Reader 2	3.27 ± 1.08	3.27 ± 0.88	3.14 ± 0.99
Reader 3	3.55 ± 1.14	3.41 ± 1.14	3.59 ± 1.18
Conspicuity left lobe			
Average*	3.12 ± 0.87	2.98 ± 0.83	2.82 ± 0.82
Reader 1*$^+$	3.55 ± 0.91	3.00 ± 1.07	2.77 ± 0.97
Reader 2	3.00 ± 0.82	3.14 ± 0.77	2.95 ± 0.79
Reader 3	2.82 ± 1.18	2.82 ± 1.05	2.73 ± 0.98
Motion robustness			
Average	3.32 ± 0.58	3.21 ± 0.47	3.20 ± 0.44
Reader 1	3.95 ± 0.65	3.91 ± 0.61	3.86 ± 0.56
Reader 2	2.64 ± 0.79	2.55 ± 0.74	2.36 ± 0.66
Reader 3	3.36 ± 0.95	3.18 ± 0.80	3.36 ± 0.85

* mb2-DWI had significantly higher score for overall image quality compared to c-DWI for scores averaged over the three readers ($p = 0.01$) and for reader 1 ($p = 0.04$). In addition, scores for conspicuity of the left lobe were also significantly higher with mb2-DWI when averaged ($p = 0.005$) and for reader 1 ($p < 0.001$). Score for right lobe sharpness ($p = 0.031$) was also significantly higher with mb2-DWI compared to c-DWI for reader 1. There were no other significant differences ($p > 0.05$) between mb2-DWI and c-DWI

$^+$There were no other significant differences between mb2-DWI and mb-DWI ($p > 0.05$) except for conspicuity of left lobe for reader 1 ($p = 0.001$)

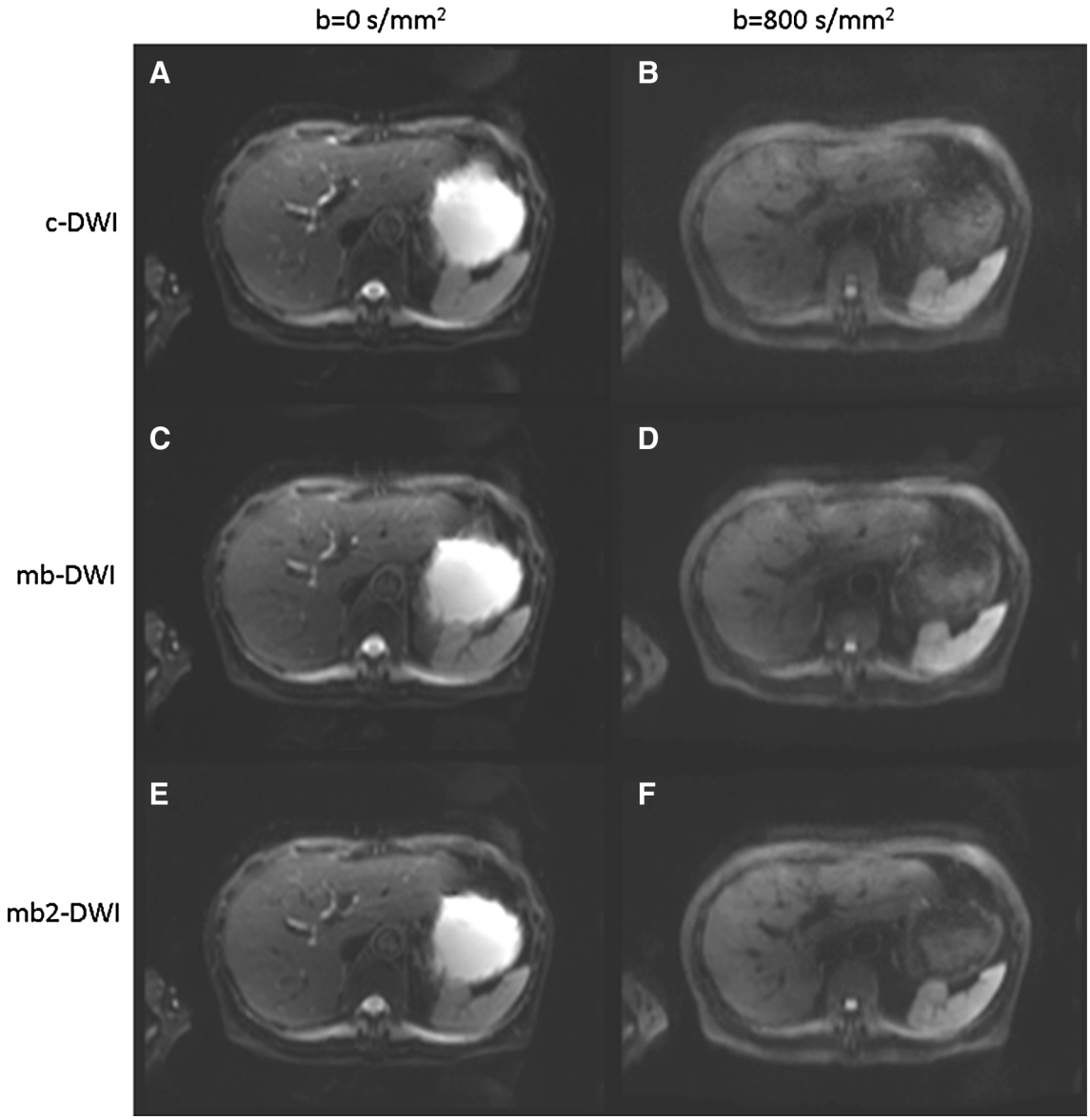

Fig. 2. 67-year-old female with history of pancreatic cystic lesion underwent diffusion-weighted imaging with conventional DWI (**A** and **B**), multiband diffusion-weighted imaging without acceleration (**C** and **D**), and multiband DWI with twofold acceleration (**E** and **F**).

$p = 0.001$) and for $b = 800$ s/mm^2 (3.24 ± 0.76 vs. 3.06 ± 0.86; $p = 0.010$).

Sharpness of the right hepatic lobe edge was also higher with mb2-DWI compared to c-DWI for $b = 0$ s/mm^2 (3.80 ± 0.79 vs. 3.61 ± 0.72; $p = 0.067$) and $b = 800$ s/mm^2 (3.76 ± 1.0 vs. 3.61 ± 1.04; $p = 0.071$), but this did not reach statistical significance.

Conspicuity of the left lobe at $b = 800$ s/mm^2 was significantly higher with mb2-DWI compared to convention c-DWI. (3.12 ± 0.87 vs. 2.82 ± 0.82; $p = 0.005$). However, there was no significant difference for $b = 0$ s/mm^2 acquisition between mb2-DWI and c-DWI (3.53 ± 0.63 vs. 3.48 ± 0.62; $p = 0.330$).

There were no significant differences with respect to clarity of the intrahepatic vessels or perceived motion robustness between mb2-DWI and c-DWI as noted in Tables 2 and 3 (Figs. 2 and 3).

Multiband with (mb2-DWI) and without acceleration (mb-DWI)

There were no significant difference in overall image quality for accelerate vs. non-accelerate (mb-2 vs. mb) schemes for $b = 0$ s/mm^2 (3.48 ± 0.52 vs. 3.33 ± 0.62; $p = 0.096$) and $b = 800$ s/mm^2 (3.24 ± 0.76 vs. 3.23 ± 0.68; $p = 0.695$). However, mb2-DWI demonstrated

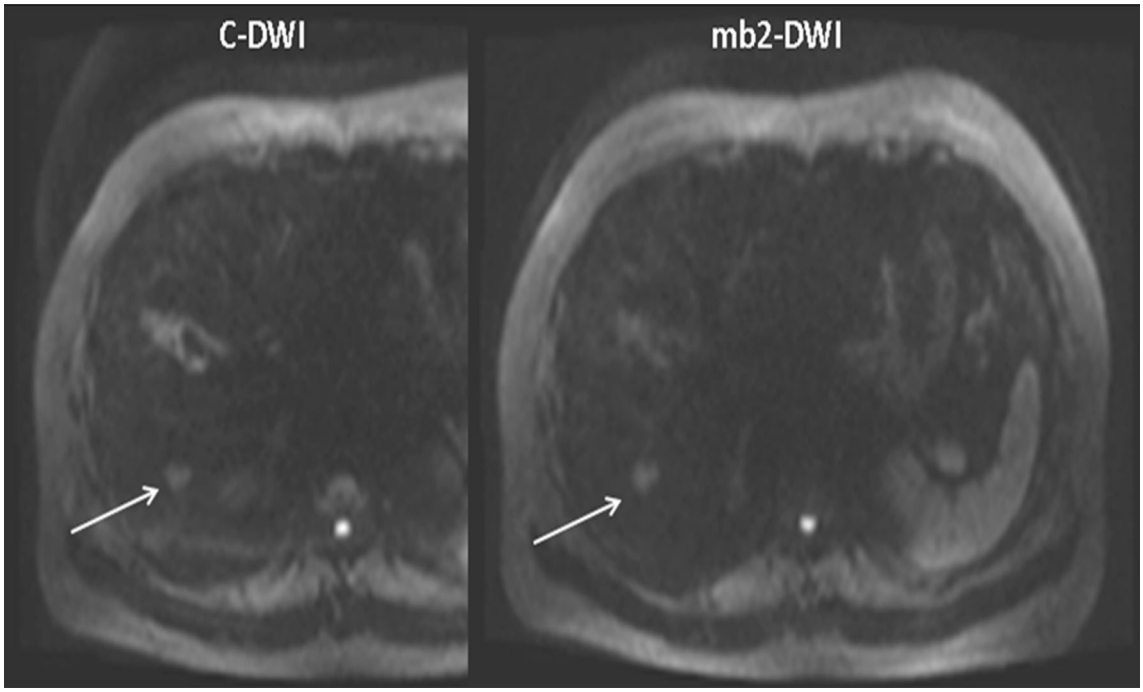

Fig. 3. 48-year-old male with history of chronic hepatitis B and cirrhosis. *b* 800 s/mm^2 image from (**A**) c-DWI and (**B**) mb2-DWI acquisitions demonstrates 1 cm hyperintense lesion in the posterior right hepatic lobe. This lesion was characterized as a hepatocellular carcinoma on dynamic pre- and post-contrast images.

improved motion robustness compared to mb-DWI for b = 0 s/mm^2 (3.20 ± 0.52 vs. 3.06 ± 0.49; $p = 0.035$) but not *b*-800 s/mm^2 (3.32 ± 0.58 vs. 3.21 ± 0.47; $p = 0.490$). Other parameters of image quality were not significantly different between the acquisitions as noted in Tables 2 and 3.

Lesion detectability

A total of same 25 lesions (greater than 5 mm in size) in 8 patients were identified on all three DWI sequences (Fig. 3). Five patients had single lesions while the remaining 3 patients had multiple lesions.

Quantitative assessment

There was no significant difference in liver SI between mb-DWI and c-DWI for $b = 0$ ($p = 0.07$) and $b = 800$ s/mm^2 ($p = 0.28$). However, liver SI was significantly lower for mb2-DWI when compared to mb-DWI and c-DWI for $b = 0$ (all $p < 0.001$) and b = 800 s/mm^2 (all $p < 0.001$) (Table 4).

ADC values of the liver for mb2-DWI, mb-DWI, c-DWI are 1.131 ± 0.139, 1.240 ± 0.129, 1.171 ± 0.151 × 10^{-3} mm^2/sec, respectively. There was no significant difference between liver ADC between mb2-DWI and c-DWI ($p = 0.12$). Bland–Altman plot (Fig. 4a, B) demonstrated slight lower liver ADC with mb2-DWI compared to c-DWI (0.043 × 10^{-3} mm^2/s) as well as mb-DWI (0.109 × 10^{-3} mm^2/s).

Table 4. Signal Intensity (SI) of the liver at $b = 0$ and $b = 800$ s/mm^2 (measured in arbitrary units) for the three diffusion sequences

Signal intensity ± SD	mb2-DWI	mb-DWI	c-DWI
b 0 s/mm^2	38.5 ± 22.1	50.9 ± 27.4	49.1 ± 25.3
b 800 s/mm^2	15.4 ± 9.4	19.8 ± 12.2	20.3 ± 12.3

Liver Signal Intensity of the mb2-DWI was significantly lower than mb-DWI and c-DWI for $b = 0$ s/mm^2 and $b = 800$ s/mm^2 (all $p < 0.001$). However, there was no significant difference in liver SI between mb-DWI and c-DWI for $b = 0$ ($p = 0.07$) and $b = 800$ s/mm^2 ($p = 0.28$)

Discussion

Our study demonstrates multiband sequence with acceleration factor of 2 (mb2-DWI) decreases acquisition time by approximately 40%–50% compared to conventional diffusion-weighted acquisition while maintaining diagnostic image quality. Despite shorter acquisition time, mb2-DWI had higher scores for overall image quality compared to c-DWI, both at $b = 0$ s/mm^2 and at $b = 800$ s/mm^2. ADC values of the liver between mb2-DWI and c-DWI were not significantly different, although ADC was slightly lower with mb2-DWI. Furthermore, there was no difference in lesion detectability between mb2-DWI and c-DWI, These results are very promising and may allow for more efficient

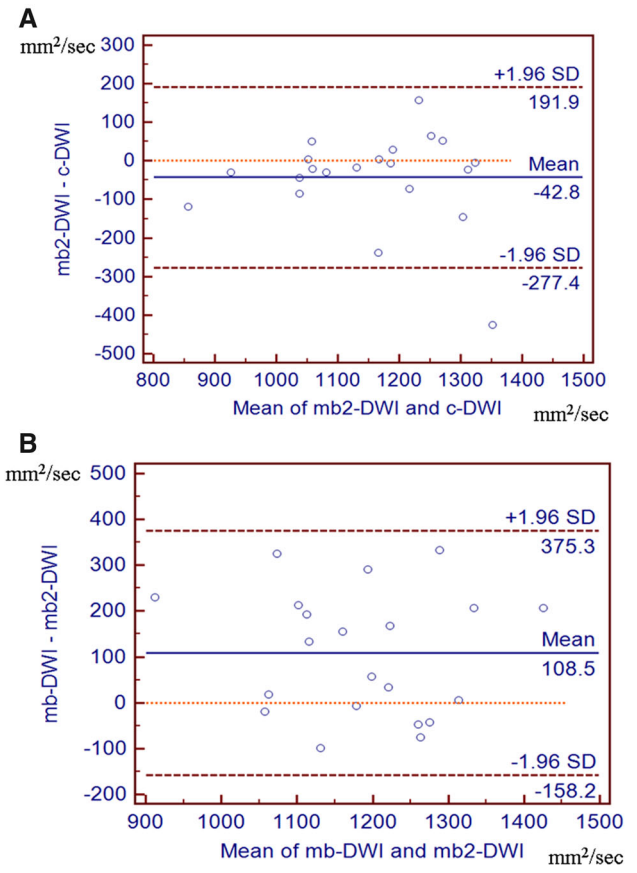

Fig. 4. Bland–Altman plot comparing ADC values of the liver between (**A**) mb2-DWI and c-DWI and (**B**) mb-DWI and mb2-DWI. This showed slight lower ADC with mb2-DWI compared to c-DWI (0.043×10^{-3} mm^2/s or 3.7% of the average ADC) and mb-DWI (0.109×10^{-3} mm^2/s or 9.4% of the average ADC).

free-breathing DWI of the abdomen. The time saving obtained with multiband DWI can either be used to decrease the total exam time, or improve volumetric coverage.

In conventional diffusion acquisition a single slice is excited, whereas in multiband diffusion multiple slices are excited simultaneously, and the corresponding readout contains these multiple slices. Using a technique called blipped CAIPIRINHA the reconstruction algorithm can separate the multiple slices that were acquired simultaneously [18]. This permits the TR to be decreased thus shortening the acquisition time. In our study, an acceleration factor of 2 allowed for two transverse slices to be acquired simultaneously thus permitting TR reduction. TR was decreased compared to c-DWI but was not minimized to allow for sufficient T1 recovery.

We also in this study compared mb2-DWI to mb-DWI, which is a multiband sequence without acceleration. However, in clinical practice there is no reason to use a multiband approach without acceleration (i.e., without TR reduction). The purpose of using mb-DWI without acceleration in our study was to understand the effects of shorter TR which is achieved with mb2-DWI. While comparing mb2-DWI with acceleration factor of two to mb-DWI without acceleration, we noted shorter acquisition time and higher motion robustness at $b = 0$ s/mm^2.

Although, we had relatively small number of patients with lesions, same 25 lesions were visualized on the three diffusion sequences. Hence, there was no overall loss of diagnostic capabilities with mb2-DWI compared to c-DWI. ADC of the liver was lower with mb2-DWI compared to the c-DWI and mb-DWI, although these differences were not statistically significant. It is not clear if this is due to lower signal intensity with mb2-DWI due to decreased TR. We compared the signal intensity of the liver on 3-diffusion sequences which were sequentially acquired. As expected the liver signal intensity was significantly lower with mb2-DWI compared to mb-DWI and c-DWI. However, despite this lower signal intensity, diagnostic image quality was maintained with mb2-DWI.

As an alternative to multiband acquisition, time is typically reduced using parallel imaging with conventional diffusion sequence. Parallel imaging can reduce number of phase encoding steps by a factor of 2–3, thus reducing EPI readout or the echo train length [20–22]. However, this reduction in echo train length does not result in significant reduction in acquisition time due to large fixed diffusion encoding time blocks [18]. Multiband can reduce scan time in addition to conventional parallel imaging because it reduces the number of diffusion encodings which are time consuming components of diffusion image acquisition thus providing the time efficiency beyond that of parallel imaging.

There are several limitations in our study, including small number of patients and lesions. Image quality was scored subjectively by the three readers. There was poor to moderate inter-reader agreement between the readers. This may reflect the readers comfort level and experience with DWI as well as intrinsic limitation of qualitative assessment of image quality. We did not perform correction for multiple comparisons despite the large number of tests that were conducted in order to maintain maximal statistical power to detect any real differences that may exist. This was considered important since the objective of this study was to assess if multiband sequence has impact on image quality rather than identify the specific aspects of image quality that are actually improved. Specifically, while failure to correct for multiple comparisons implies that certain aspects of image quality identified as different may be false positives, the fact that many of the image quality parameters are not significantly different between mb2-DWI and c-DWI remains valid. Larger study with higher statistical power will be required to tease out which of the differences are truly significant. We did not perform quantitative measurement or estimation of signal-to-noise ratio (SNR) in

our study due to difficulties with noise measurement with use of parallel imaging. Instead, we measured liver signal intensity on $b = 0$ and $b = 800$ s/mm^2 as well as ADC of the liver, and compared these between the three sequences. We did not assess the differences in lesion conspicuity between different sequences. Larger study demonstrating non-inferiority in lesion detectability with mb2-DWI compared to c-DWI would be helpful. Although decreasing acquisition time by 40%–50% for a single station has relatively small impact on overall acquisition time for liver MR examination, use of this technique can substantially lower acquisition time in patients undergoing multi-station exam or whole-body diffusion either with or without simultaneous PET exam (PET-MR).

In conclusion, multiband technique with an acceleration factor of 2 can provide nearly twofold acceleration with maintained or higher overall image quality compared to conventional free-breathing diffusion-weighted imaging of the abdomen with identical lesion detectability. Thus, mb2-DWI can potentially replace the conventional diffusion-weighted acquisition in the liver.

Acknowledgment. Kawin Setsompop, Ph.D. Stephen F. Cauley, Ph.D. Athinoula A. Martinos Center for Biomedical Imaging, Department of Radiology, Massachusetts General Hospital, Charlestown, Massachusetts, USA.

References

1. Bharwani N, Koh DM (2013) Diffusion-weighted imaging of the liver: an update. Cancer Imaging 13:171–185
2. d'Assignies G, Fina P, Bruno O, et al. (2013) High sensitivity of diffusion-weighted MR imaging for the detection of liver metastases from neuroendocrine tumors: comparison with T2-weighted and dynamic gadolinium-enhanced MR imaging. Radiology 268(2):390–399
3. Taouli B, Ehman RL, Reeder SB (2009) Advanced MRI methods for assessment of chronic liver disease. Am J Roentgenol 193(1):14–27
4. Namimoto T, Yamashita Y, Sumi S, Tang Y, Takahashi M (1997) Focal liver masses: characterization with diffusion-weighted echo-planar MR imaging. Radiology 204(3):739–744
5. Kim T, Murakami T, Takahashi S, et al. (1999) Diffusion-weighted single-shot echoplanar MR imaging for liver disease. Am J Roentgenol 173(2):393–398
6. Cui Y, Zhang XP, Sun YS, Tang L, Shen L (2008) Apparent diffusion coefficient: potential imaging biomarker for prediction and early detection of response to chemotherapy in hepatic metastases. Radiology 248(3):894–900
7. Parikh T, Drew SJ, Lee VS, et al. (2008) Focal liver lesion detection and characterization with diffusion-weighted MR imaging: comparison with standard breath-hold T2-weighted imaging. Radiology 246(3):812–822
8. Taouli B, Koh DM (2010) Diffusion-weighted MR Imaging of the Liver. Radiology 254(1):47–66
9. Taouli B, Sandberg A, Stemmer A, et al. (2009) Diffusion-weighted imaging of the liver: comparison of navigator triggered and breathhold acquisitions. J Magn Reson Imaging 30(3):561–568
10. Bruegel M, Holzapfel K, Gaa J, et al. (2008) Characterization of focal liver lesions by ADC measurements using a respiratory triggered diffusion-weighted single-shot echo-planar MR imaging technique. Eur Radiol 18(3):477–485
11. Asbach P, Hein PA, Stemmer A, et al. (2008) Free-breathing echo-planar imaging based diffusion-weighted magnetic resonance imaging of the liver with prospective acquisition correction. J Comput Assist Tomo 32(3):372–378
12. Choi JS, Kim MJ, Chung YE, et al. (2013) Comparison of breathhold, navigator-triggered, and free-breathing diffusion-weighted MRI for focal hepatic lesions. J Magn Reson Imaging 38(1):109–118
13. Chen X, Qin L, Pan D, et al. (2014) Liver diffusion-weighted MR imaging: reproducibility comparison of ADC measurements obtained with multiple breath-hold, free-breathing, respiratory-triggered, and navigator-triggered techniques. Radiology 271(1):113–125
14. Kwee TC, Takahara T, Koh DM, Nievelstein RAJ, Luijten PR (2008) Comparison and reproducibility of ADC measurements in breathhold, respiratory triggered, and free-breathing diffusion-weighted mr imaging of the liver. J Magn Reson Imaging 28(5):1141–1148
15. Nasu K, Kuroki Y, Fujii H, Minami M (2007) Hepatic pseudo-anisotropy: a specific artifact in hepatic diffusion-weighted images obtained with respiratory triggering. Magn Reson Mater Phys 20(4):205–211
16. Feinberg DA, Setsompop K (2013) Ultra-fast MRI of the human brain with simultaneous multi-slice imaging. J Magn Reson 229:90–100
17. Lau AZ, Tunnicliffe EM, Frost R, Koopmans PJ, Tyler DJ, Robson MD (2015) Accelerated human cardiac diffusion tensor imaging using simultaneous multislice imaging. Magn Reson Med 73(3):995–1004
18. Setsompop K, Gagoski BA, Polimeni JR, et al. (2012) Blipped-controlled aliasing in parallel imaging for simultaneous multislice echo planar imaging with reduced g-factor penalty. Magnet Reson Med 67(5):1210–1224
19. Landis JR, Koch GG (1977) The measurement of observer agreement for categorical data. Biometrics 33(1):159–174
20. Griswold MA, Jakob PM, Heidemann RM, et al. (2002) Generalized autocalibrating partially parallel acquisitions (GRAPPA). Magn Reson Med 47(6):1202–1210
21. Pruessmann KP, Weiger M, Scheidegger MB, Boesiger P (1999) SENSE: sensitivity encoding for fast MRI. Magn Reson Med 42(5):952–962
22. Sodickson DK, Manning WJ (1997) Simultaneous acquisition of spatial harmonics (SMASH): Fast imaging with radiofrequency coil arrays. Magn Reson Med 38(4):591–603